Solid-State Nuclear Magnetic Resonance Techniques for the Structural Characterization of Geminal Alane-Phosphane Frustrated Lewis Pairs and Secondary Adducts

Anna-Lena Wübker[+],[a] Jonas Koppe[+],[a] Henrik Bradtmüller[+],[a, c] Lukas Keweloh,[b] Damian Pleschka,[b] Werner Uhl,*[b] Michael Ryan Hansen,*[a] and Hellmut Eckert*[a, d]

Abstract: The first comprehensive solid-state nuclear magnetic resonance (NMR) characterization of geminal alane-phosphane frustrated Lewis pairs (Al/P FLPs) is reported. Their relevant NMR parameters (isotropic chemical shifts, direct and indirect ^{27}Al-^{31}P spin-spin coupling constants, and ^{27}Al nuclear electric quadrupole coupling tensor components) have been determined by numerical analysis of the experimental NMR line shapes and compared with values computed from the known crystal structures by using density functional theory (DFT) methods. Our work demonstrates that the ^{31}P NMR chemical shifts for the studied Al/P FLPs are very sensitive to slight structural inequivalences. The ^{27}Al NMR central transition signals are spread out over a broad frequency range ($>$ 200 kHz), owing to the presence of strong nuclear electric quadrupolar interactions that can be well-reproduced by the static ^{27}Al wideband uniform rate smooth truncation (WURST) Carr-Purcell-Meiboom-Gill (WCPMG) NMR experiment. ^{27}Al chemical shifts and quadrupole tensor components offer a facile and clear distinction between three- and four-coordinate aluminum environments. For measuring internuclear Al···P distances a new resonance-echo saturation-pulse double-resonance (RESPDOR) experiment was developed by using efficient saturation via frequency-swept WURST pulses. The successful implementation of this widely applicable technique indicates that internuclear Al···P distances in these compounds can be measured within a precision of ± 0.1 Å.

[a] A.-L. Wübker,[+] Dr. J. Koppe,[+] Dr. H. Bradtmüller,[+] Prof. M. R. Hansen, Prof. H. Eckert
Institut für Physikalische Chemie
WWU Münster
Corrensstraße 28/30, 48149 Münster (Germany)
E-mail: mhansen@uni-muenster.de
         eckerth@uni-muenster.de

[b] Dr. L. Keweloh, Dr. D. Pleschka, Prof. W. Uhl
Institut für Anorganische und Analytische Chemie
WWU Münster
Corrensstraße 28/30, 48149 Münster (Germany)
E-mail: uhlw@uni-muenster.de

[c] Dr. H. Bradtmüller[+]
Department of Materials Engineering
Vitreous Materials Laboratory
Federal University of São Carlos
CP 676, 13565-905, São Carlos, SP (Brazil)

[d] Prof. H. Eckert
Instituto de Física de São Carlos
Universidade de São Paulo
São Carlos SP 13566-590 (Brazil)

[+] These authors contributed equally to this work.

📖 Supporting information for this article is available on the WWW under https://doi.org/10.1002/chem.202102113

Introduction

During the past decade, frustrated Lewis pairs (FLPs) have gained considerable attention as versatile metal-free reagents applicable in various important chemical processes such as adduct formation, activation, or cooperative catalytic transformations.[1–7] FLPs are chemical systems containing a Lewis base as well as a Lewis acid moiety in close proximity, where the formation of a chemical bond ("quenching") is not a thermodynamic sink as a result of the presence of sterically demanding substituents at the Lewis centers. Such "frustration" bestows important catalytic properties on these molecules, resulting from the cooperative action of the Lewis centers upon the substrate molecule. Among this class of substances, intramolecular FLPs with an electron-poor borane and an electron-rich phosphane functionality (B/P-FLPs) are particularly prominent as they allow for instance the activation of small unreactive molecules such as dihydrogen or carbon dioxide.[8–12] Solid-state NMR techniques have been extensively used to describe the structural properties of these materials,[13] characterize their degree of frustration,[14] which correlates with their reactivity, and to characterize the stereochemistry[15] and aggregation phenomena[16] of FLPs with molecular substrates.

Besides the widely studied borane-phosphane FLPs, the alane-phosphane homologs present a viable alternative in chemical reactivity and homogeneous FLP catalysis.[17–23] With few exceptions[20–23] the field of intramolecular Al/P systems has been focusing on geminal compounds,[19,24–52] where the relative orientation of the orbitals limits the degree of possible overlap,

Chemistry–A European Journal

Full Paper
doi.org/10.1002/chem.202102113

Chemistry Europe
European Chemical
Societies Publishing

rendering these generally more reactive in comparison to borane-phosphane FLPs. To the best of our knowledge, solid-state NMR techniques have never been used for the structural characterization of these systems. A major impediment for such studies has been the interaction of the ^{27}Al nuclear electric quadrupole moments with the large local electric-field gradients (EFGs) created by the trigonal or strongly distorted fourfold Al coordination environments found in such compounds. In this case, the anisotropy of the nuclear electric quadrupolar interactions produces NMR line shapes that are broadened over wide frequency ranges exceeding the limited excitation window available with standard NMR probe equipment and rectangular radio-frequency (rf) pulses. A new approach to this problem has been offered by recent developments in ultra-wideline methodologies:[53–58] The combination of Carr-Purcell-Meiboom-Gill (CPMG) acquisition[59,60] and wide-band uniform-rate smooth truncation (WURST)[55–58] pulses for frequency-swept excitation and refocusing offers the measurement of undistorted NMR line shapes spanning several MHz. Using this advanced WCPMG technique, the present contribution details the first comprehensive characterization of a group of geminal phosphane-alane molecules by ^{27}Al and ^{31}P solid-state NMR. We present appropriate experimental conditions to record high-fidelity ^{27}Al NMR line shapes and examine the informational content of the NMR parameters, i.e. the isotropic chemical shift, nuclear electric quadrupole coupling tensor components, and indirect ^{31}P-^{27}Al spin-spin coupling constants based on DFT calculations. Previous work on borane-phosphane FLPs had also indicated the potential of ^{31}P/^{11}B double-resonance NMR techniques such as rotational echo double resonance (REDOR)[61] or rotational echo adiabatic passage double resonance (REAPDOR)[62] for measuring interatomic B···P distances.[13–16] However, these techniques are rendered ineffective due to the wide ^{27}Al frequency dispersion caused by strong quadrupole interactions for which, in particular, the NMR frequencies of the satellite transitions are dispersed over several MHz. Recently, new wideband dipolar recoupling techniques based on the application of more advanced rf pulse concepts have been developed for such situations. For example, an extension of the resonance echo saturation-pulse double-resonance (RESPDOR) method,[63,64] which uses phase-modulated (PM) saturation pulses for effective recoupling of nuclei resonating over a wide frequency region, has already been successfully demonstrated on various model systems.[65–69] Alternatively, it is expected that efficient dipolar recoupling may also be possible by integrating frequency-swept WURST pulses instead. In the present contribution, we will demonstrate the first successful application of this idea, and its use for internuclear distance measurements in alane-phosphane FLPs.

Experimental Section

Sample preparation and characterization: Scheme 1 summarizes the alane-phosphane FLP systems characterized in this study. The syntheses of these compounds and their crystallographic characterization were previously described.[29,32,36,39] The materials have closely related molecular structures, showing only small variations
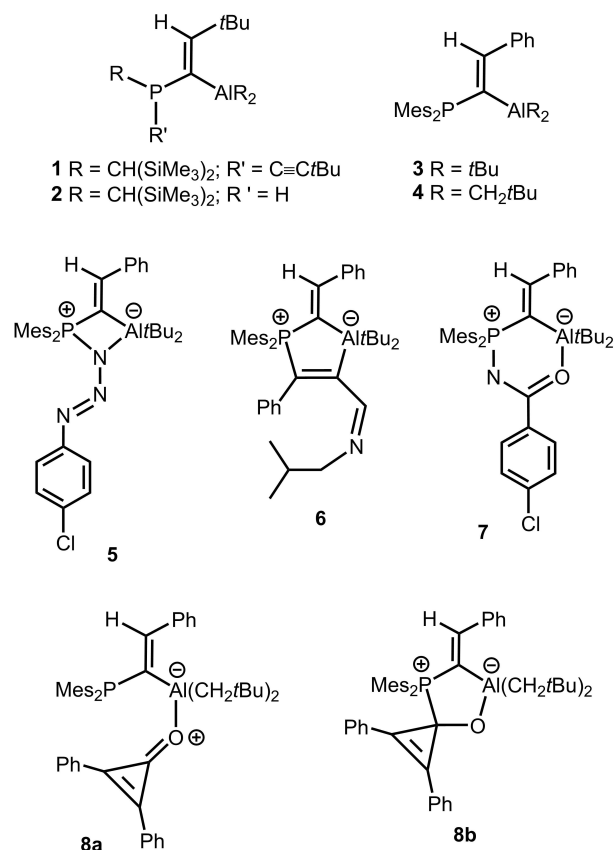
Scheme 1. Molecular structures of the alane-phosphane FLP compounds studied in this work. The abbreviation "Mes" denotes a mesitylene (1,3,5 trimethylphenyl) ligand.

of their molecular backbones. All systems are geminal (1,3) phosphane alanes. Molecules **1–4** have three-coordinated Al atoms, while in molecules **5–8** the coordination number at the Al site is four. Compound **8** is a particularly special case, containing both the cyclic and the non-cyclic isomer within the same crystal structure.[32]

Solid-State NMR spectroscopic characterization: Measurements were carried out using Bruker Avance-III-300 and Avance-I-400 spectrometers operating at magnetic field strengths of 7.05 and 9.4 T, respectively. All experiments were performed with 4 mm double- and triple-resonance probes. For maximum resolution, we used ^{1}H heteronuclear decoupling (SW$_f$-TPPM15,[67] $\nu_{RF} = 52$–70 kHz).

The ^{31}P{^{1}H} cross-polarization MAS (CP/MAS) NMR experiments were conducted using a 5.0 μs π/2 pulse on ^{1}H ($\nu_{RF} = 50$ kHz) for excitation followed by a 2–3 ms spin-lock pulse ramped on ^{1}H from 70 to 100 % to a maximum nutation frequency between 55 and 75 kHz. The nutation frequency (power level) on the ^{31}P channel was optimized with respect to maximum signal intensity. A recycle delay of 5–10 s proved to be sufficient. All ^{31}P NMR spectra are referenced to 85 % H$_3$PO$_4$ solution. Static ^{27}Al{^{1}H} WCPMG NMR experiments were conducted using a 30–50 μs pulse with a shape parameter of 80 and sweep widths between 0.6 and 1 MHz. Details of the experimental conditions are summarized in Table S1. The delay before and after the WURST pulse was set to 10–20 μs and a recycle delay to 1–2 s was used. All ^{27}Al WCPMG NMR spectra were referenced to a 1 M aqueous solution of aluminum nitrate. The ^{31}P{^{27}Al} dipolar recoupling experiments were conducted using the RESPDOR sequence at 7.05 T and $\nu_{MAS} = 10$ kHz on the Bruker Avance-III-300 spectrometer, using a commercially available 4 mm

Chemistry–A European Journal

Full Paper
doi.org/10.1002/chem.202102113

Chemistry Europe
European Chemical
Societies Publishing

Table 1. Experimental and calculated NMR parameters for compounds **1–8**.. For compound **4**, the second entry refers to a single-molecule calculation.

	C_Q (calc)/ MHz	C_Q (exp)/ MHz ±0.2	η_Q (calc)	η_Q (exp) ±0.05	δ (^{27}Al) (calc)/ppm	δ (^{27}Al) (exp)/ppm ±5	$\delta(^{31}$P) (calc)/ppm	$\delta(^{31}$P) (exp)/ppm ±0.2	d(Al–P) (cryst.)/Å	J(Al–P) (calc)/Hz	J(Al–P) (exp)/Hz ±0.5
1	38.83	39.9	0.057	0.04	255.37	221	−57.5	−54.4	3.4285	−8.033	
	38.84		0.057		255.03		−60.9	−55.6	3.4285	−8.031	
2	38.98	40.1	0.068	0.06	258.40	190	−62.0	−65.5/−65.9	3.3409	20.591	25.6/13.8
	39.36	40.7	0.040	0.04	262.67	200	−81.6	−83.1/−83.3	3.3409	−7.511	7.5/7.5
3	42.09	43.4	0.196	0.21	238.05	222	−4.0	−13.8	3.2834	44.179	43.6
	43.42		0.210		253.94		−5.7	−14.6	3.2898	43.108	43.7
4	42.98	43.9	0.192	0.22	251.20	250	−13.0	−33.3	3.1935	44.998	
	42.99		0.128		254.70		−19.4			5.960	
5	20.68	21.3	0.722	0.69	163.33	165	35.5	40.3	2.8150	6.166	
6	14.41	14.3	0.667	0.65	155.55	150	29.7	29.4	3.1260	19.006	
7	17.49	18.2	0.779	0.78	136.80	135	30.9	35.9	3.2795	3.522	
8a	22.43	17.0	0.340	0.39	147.85	150	6.4	−8.9	3.2232	26.903	
8b	15.48	11.0	0.542	0.55	145.55	100	23.1	27.5	3.1514	14.919	

triple-resonance MAS probe. The experiments employed two different ^{27}Al saturation pulse schemes, based on the PM-saturation[64] and the WURST[53] pulse concepts. ^{31}P excitation was achieved by cross-polarization with a 3 μs π/2 pulse on ^{1}H ($\upsilon_{RF}(^1H) = 83.33$ kHz) and a pulse ramped from 90 to 100% of the amplitude required to fulfill the HARTMANN-HAHN matching condition. The ^{31}P nutation frequency ν_{RF} was 50 kHz. The WURST saturation pulse was applied over a length of 12 rotorcycles (1.2 ms) with a shape parameter of 80, a sweep width of 450 kHz, and a nutation frequency between 27 and 32 kHz. As a reference experiment recoupling with PM-RESPDOR was carried out, employing the PM saturation pulses for 10 cycles (1.0 ms). However, due to strong power reflections, the input power was restricted to rf amplitudes corresponding to nutation frequencies between 19 and 21 kHz. Recycle delays varied between 5 and 10 s, and a ^{1}H saturation comb of 60 pulses with identical pulse lengths as for excitation was used prior to every experiment. During the ^{31}P π-pulse trains and acquisition, ^{1}H SW$_f$-TPPM[71] decoupling was used with ^{1}H rf power corresponding to a nutation frequency of 50 kHz. All the simulations of spectra and RESPDOR experiments were carried out using the SIMPSON software.[72]

DFT calculations: All the DFT calculations were carried out under gas-phase conditions with Turbomole,[73,74] Gaussian,[75] and Orca.[76] The DFT calculations are based on the molecular structures obtained either from single-crystal X-ray diffraction or by energy optimization of isolated molecules in the gas phase, where the hydrogen atomic positions were optimized. In some cases both approaches were compared. The geometry optimizations were performed with TURBOMOLE, a def2-TZVP basis set[77] including D3 dispersion correction[78,79] and the TPSS-functional[80] on a meta-GGA level. Geometry optimizations and the SCF cycles were set to $5 \cdot 10^{-7}$ E_H and 10^{-7} E_H, respectively, as energy-convergence criteria. The *Resolution of Identity* (RI) approximation[81,82] was applied and the integration grid was set to *m4*.[76] For compound **4** one additional geometry optimization was performed based on the molecular structure created with ChemDraw. This additional geometry optimization was performed with Orca, a def2-TZVP basis set including D3 dispersion correction with Becke-Johnson damping and the PBE0-functional on a hybrid-GGA level.
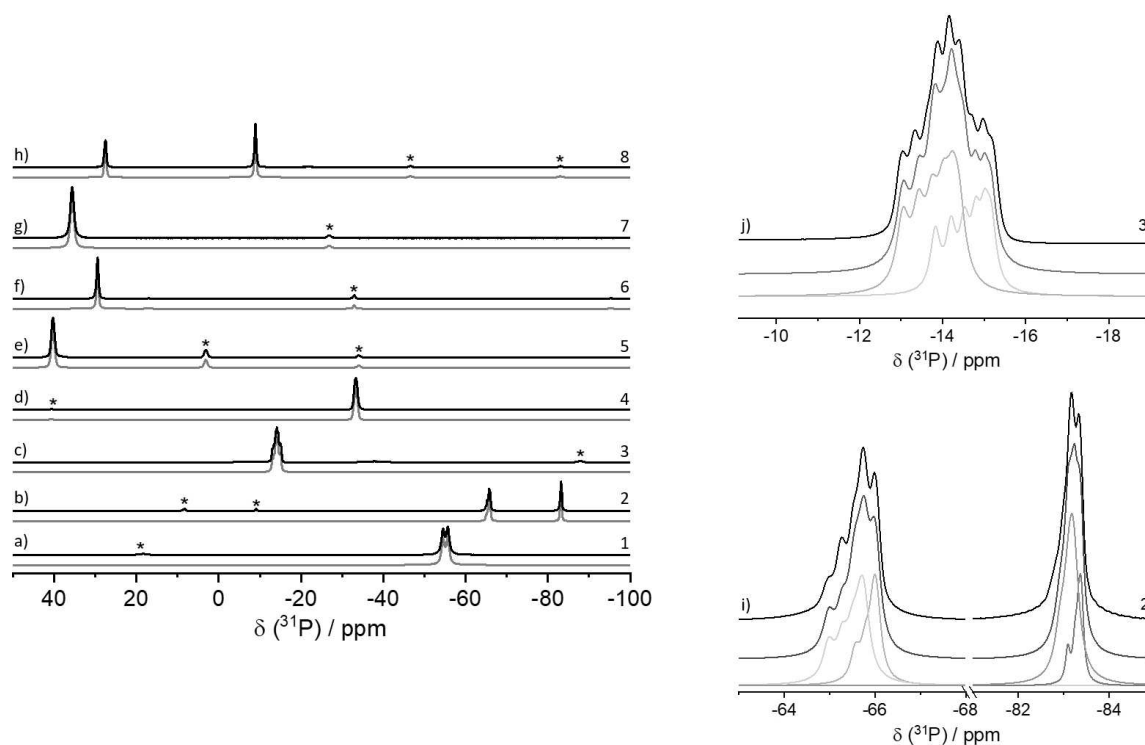
Magnetic shielding parameters were calculated using TURBOMOLE, a def2-TZVP basis set, and the B3LYP[83,84] hybrid functional by application of the *Gauge Invariant Atomic Orbitals approach*.[85,86] NMR chemical shifts were referenced to phosphoric acid and aluminum nitrate ($\delta_{iso} = \sigma_{ref}^{calc} - \sigma_{sample}^{calc}$). For the reference compounds the calculation resulted in $\sigma_{H_3PO_4} = 272.28$ ppm and $\sigma_{Al(NO_3)_3} = 558.59$ ppm.

The ^{27}Al quadrupolar coupling parameters (C_Q and η_Q) were calculated using GAUSSIAN and the GGA functional B97-D.[87] The applied def2-TZVP basis set was expanded using additional functions of the cc-pCVTZ basis set from the EMSL database[88,89] with large exponents; for details refer to Ref. [13]. Quadrupolar coupling parameters were extracted from this data using the program EFGShield (VERSION V4.0).[90] ^{27}Al–^{31}P indirect spin-spin-(J)-coupling constants were calculated in GAUSSIAN using a TZVP basis set and the B3LYP functional.

Results and Discussion

Characterization of the phosphorus environments using ^{31}P {^{1}H} CP MAS NMR

Figure 1a)–h) and Table 1 summarize the ^{31}P MAS NMR results. In compounds with two crystallographically distinct P atoms (compounds **1–3** and **8**), separate ^{31}P resonances with approximately equal intensities are observed, although the close overlap of the signals in **1** and **3** indicate that the structural differences are rather subtle. For compounds **1** and **2**, the measured ^{31}P chemical shifts are found in good agreement with the DFT-calculated values, whereas in compounds **3** and **4** somewhat larger deviations are found. In compounds **8a** and **8b**, the cyclic and open-chain isomers are easily differentiated, confirming previous preliminary results.[32] Table 1 further indicates that the calculated ^2J(P–Al) values in the present compounds vary between 0 and 45 Hz. Whether or not this indirect spin-spin interaction can also be experimentally detected depends on the spin-lattice relaxation times of the ^{27}Al nuclei, which govern the lifetimes of the corresponding Zeeman states. In the present series, we observe J-splitting only in compounds **2** and **3**. In the case of compound **3**, we observe two equally intense closely overlapping J-multiplets belonging to two crystallographically distinct molecules. From the optimized simulation (Figure 1b), performed with the DMfit program,[91] we extract a $^2J(^{31}$P-^{27}Al) isotropic indirect spin-spin coupling constant of ~43 Hz, which is in excellent agreement with the value determined from the DFT calculation. The line shape of the J-splitting pattern (Figure 1i) is further influenced by a cross-term between the dipolar and quadrupolar inter-

Chemistry–A European Journal

Full Paper
doi.org/10.1002/chem.202102113

Chemistry
Europe
European Chemical
Societies Publishing

Figure 1. $^{31}P\{^1H\}$CP/MAS NMR spectra of compounds **1**–**8**. a)–d): compounds with three-coordinate Al; e)–h): compounds with four-coordinate Al; spinning sidebands are indicated by asterisks. Horizontally expanded experimental and simulated spectra of compound **2** and **3** in i) and j), respectively, show the effect of isotropic indirect spin-spin coupling, characterized by the coupling constant $^2J(^{31}P-^{27}Al)$ on the ^{31}P spectra of the different phosphorus sites.

action-tensors that becomes relevant when the effect of the quadrupolar interaction upon the Zeeman energy levels must be described by second-order perturbation theory. The effect of this second-order shift depends on the Euler angles specifying the mutual orientations of the ^{27}Al EFG principal axes relative to the Al–P vector (α^D, β^D). The relevant Euler angles of $\alpha^D = 301.35°$ and $\beta^D = 72.52°$ were taken from the DFT calculations and used as a constraint in the simulation. Partially resolved multiplets are also observed for compound **2**. In this case ($\alpha^D = 171.50°$ and $\beta^D = 93.59°$), the corresponding $^2J(^{31}P-^{27}Al)$-coupling constants were found to be significantly smaller, as also predicted from the theoretical calculation, cf. Table 1. As expected, in both compounds **2** and **3**, the orientation of the z-axis of the ^{27}Al EFG tensor (which is approximately coincident with the pseudo-C$_3$-axis) is found to be close to orthogonal to the P–Al vector, see Scheme 1.

Characterization of the Al environments by static ^{27}Al WCPMG NMR

Figure 2 summarizes the static ^{27}Al WCPMG NMR spectra, which are shown in their static envelope representation obtained by co-addition of the individual spin echoes following the entire CPMG pulse train. These spectra can be simulated well on the basis of the quadrupolar interaction only, whose influence on the line shape is calculated using the diagonalization method via the QUEST software.[92] The ^{27}Al chemical shift anisotropy
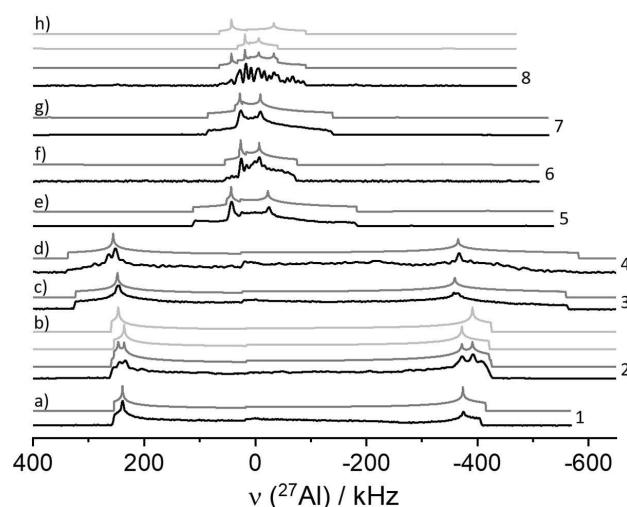
Figure 2. Static ^{27}Al WCPMG NMR spectra of compounds **1**–**8**. a)–d): compounds with three-coordinate Al; e)–h): compounds with four-coordinate Al. Black curves illustrate experimental data while grey spectra denote simulations. In case of compounds **2** (b)) and **8** (h)) two distinct simulation components are included.

$(\Delta\sigma)$[93] does not appear to have any significant influence on the static NMR line shapes. This is confirmed by the DFT calculations, indicating values of 150 ppm or less (see Table S2). Note that the two crystallographically distinct Al atoms in compound **2** are well-differentiated in the static ^{27}Al NMR line

Chemistry–A European Journal

Full Paper
doi.org/10.1002/chem.202102113

**Chemistry
Europe**
European Chemical
Societies Publishing

shapes. In contrast, in compound **3**, in which the two distinct phosphorus sites have different ^{31}P chemical shifts, the two Al sites are not resolved in the static ^{27}Al NMR spectrum. For compound **8**, the fourfold coordinated ^{27}Al nuclei of the two distinct molecules **8a** and **8b** yield a more complex NMR line shape that can be satisfactorily simulated by a superposition of two ^{27}Al central transition quadrupolar powder patterns in a 1:1 ratio. From Figure 2 and Table 1 we see that the ^{27}Al quadrupolar coupling constant and the isotropic chemical shift can differentiate rather well between three- and four-coordination at the aluminum site, in agreement with previous findings.[94] Three-coordinated Al species are characterized by C_Q-values near 40 MHz, close-to-axially symmetric EFG tensors, and isotropic chemical shifts δ near 250 ppm. In contrast, four-coordinated Al species are characterized by C_Q-values near 20 MHz, EFG asymmetry parameters η_Q larger than 0.5, and isotropic chemical shifts δ near 150 ppm. In compound **6** and the ring isomer **8b** the ^{27}Al quadrupolar coupling constants appear to be unusually small. Possibly this is a consequence of partial averaging of the electric field gradient due to some molecular motion in the solid state.

Distance measurements by ^{31}P{^{27}Al} double resonance experiments

Initial attempts to measure Al···P distances by REDOR or REAPDOR experiments for the compounds summarized in Scheme 1 were unsuccessful, which can be understood given the large spread of ^{27}Al resonance frequencies caused by the strong second-order quadrupolar perturbations affecting the spins. Therefore we used an alternative RESPDOR scheme, designed for wideband saturation:[63,64] In doing so, we implemented the frequency sweep principle of WURST pulses in the RESPDOR scheme and compared the performance of this new sequence with that of the phase-modulated saturation sequence used by Goldbourt and coworkers.[66–69]

In this phase-modulated (PM) RESPDOR NMR experiment[66] (initially referred to as PM low-alpha (LA) REDOR),[67,68] the characteristic PM-saturation pulse[69] (see Figure 3) is employed for saturation of the macroscopic magnetization associated with the S-spin ensemble that is typically exposed to a large interaction anisotropy. Nimerovsky et al. recently also considered the application of WURST pulses for the inversion of the S-spin populations;[68] however, based on their presented numerical simulations, they concluded that the inversion performance is rather non-uniform, and that an additional parameter optimization may be required. Indeed, the requirements for WURST pulses to allow an adiabatic (full) inversion of spins exposed to strong anisotropic interactions under MAS as in this work would require the use of extremely large rf-amplitudes and frequency-sweep widths that are hardly realizable in practice.[95] We note that very recent work by Venkatesh et al. has shown that short, hard adiabatic pulses (SHAPs) may be used for the adiabatic inversion of ^{195}Pt with a linewidth larger than 8000 ppm, using rf nutation frequencies beyond 250.0 kHz.[96] However, WURST pulses may in fact replace the PM pulse for saturation of the S-spin system in what we have
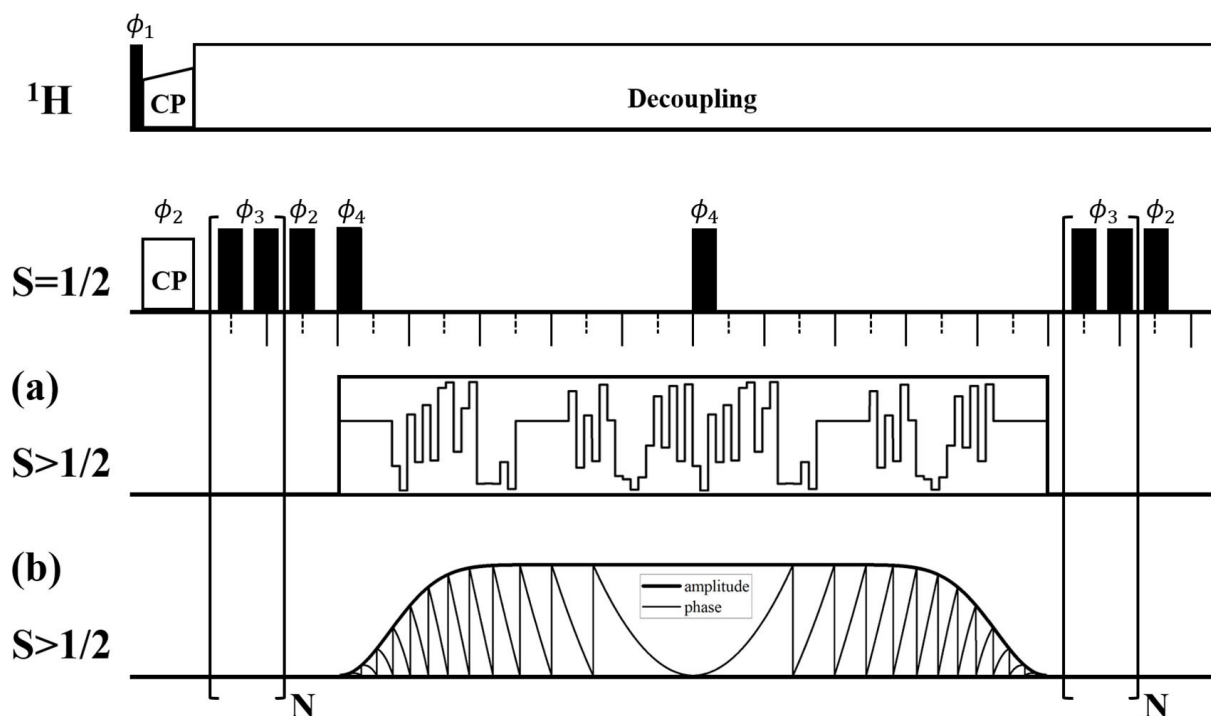

Figure 3. RESPDOR pulse sequence used in the present study for ^{27}Al (S = 5/2) dipolar recoupling of ^{31}P nuclei (S = 1/2). The bottom layers show the amplitude (envelope) and phase profiles for either the PM (a) or the WURST (b) pulses applied to the ^{27}Al nuclei. Pulse phases $\phi_1 - \phi_4$ and receiver phase can be found in Ref. [66].

Chemistry–A European Journal

Full Paper
doi.org/10.1002/chem.202102113

Chemistry Europe
European Chemical
Societies Publishing

termed the WURST-RESPDOR (W-RESPDOR) NMR experiment. The advantage of such an approach is that WURST pulses are straightforwardly implemented and easily accessible via any spectrometer software, for example, the BRUKER software program *Topspin* (using Shapetool). In contrast, the PM-saturation pulse is somewhat inconvenient and difficult to handle due to its phase-profile elements (see Figure 3) possessing building blocks of length $0.109375\tau_{rot}$ with phase settings that require the highest possible digitization for an appropriate, digitized representation of the overall PM pulse. This makes the size of the corresponding shape files large, which in some cases, in particular when older NMR hardware is employed, may cause problems related to memory allocation restrictions when recording PM-RESPDOR curves (S and S_0) with many data points in a single experiment. Moreover, the time resolution of the WURST phase profiles (linear frequency sweep corresponding to a quadratic phase profile) can be chosen according to the intended bandwidth covered by the frequency sweep (NYQUIST limit if necessary). In addition, the rounded edges of WURST pulses typically allow the application of higher rf-field strengths[70] than the PM-saturation pulses (rectangular-shaped rf-amplitude), which generally favor saturation performances, in particular for strong quadrupolar couplings.[67–69] Herein, we have evaluated the saturation performance for WURST-80 pulses with different sweep widths Δ applied to ^{27}Al ($I=5/2$) using spin-density matrix analysis (SIMPSON,[72] see Supporting Information for further details), not considering spin-lattice relaxation effects. Various combinations of the WURST-pulse lengths τ_{rf} and sweep widths Δ were investigated as summarized in Figure S1, showing that τ_{rf} should be restricted to a multiple of the rotation period, which we set to 100 μs, according to $\nu_{rot}=10$ kHz, in all simulations. Also, we only considered symmetric, positive frequency sweeps for the WURST pulses, i.e., always sweeping from $-\Delta/2 \rightarrow +\Delta/2$ about the carrier frequency $\Delta\nu=0$ (in the rotating frame). Indeed, distinct WURST-80 pulses achieve S-spin saturation as required in the RESPDOR experiment. This is demonstrated in Figure 4 for rf-amplitudes corresponding to $\nu_{RF}=50$ kHz for all pulses,

considering quadrupolar coupling constants up to $C_Q=50$ MHz. All the simulations of saturation behavior assumed axially symmetric EFG tensors.

In particular, we identified the saturation performances for WURST-80 pulses irradiated for 12 rotor periods, resulting in a pulse length of $\tau_{rf}=1200$ μs to be comparable to that of the 1000 μs PM-saturation pulse employed in PM-RESPDOR. In general, these simulations also show that achieving complete saturation is more difficult for stronger quadrupolar couplings, in agreement with prior reports.[68,69] For WURST pulses, the choice of a larger frequency-sweep width allows to extend the overall saturation performance to larger coupling strengths. However, care must be taken when choosing the exact value of Δ as can be identified from Figure 4a for sweep widths of $\Delta=$ 450, 2400, and 4500 kHz (see also Figure S1): When sweeping over 4500 kHz, the achieved S-spin saturation is comparable to that of the PM-saturation pulse over the entire range of considered quadrupolar coupling constants (C_Q). For $C_Q=$ 50 MHz, a small, residual S-spin polarization of 9% (10%) is predicted for both the WURST-80 and PM-saturation pulse. When reducing the sweep width to $\Delta=450$ kHz, the saturation performance drops notably at about $C_Q=\sim25$ MHz, but remains below 25% (see horizontal black line) for the considered range of C_Q. In contrast, when choosing $\Delta=2400$ kHz, the saturation performance decreases almost linearly with increasing C_Q, only being preferable to $\Delta=450$ kHz for $C_Q > \sim33$ MHz. In Figure 4b, we have considered the limited rf-amplitudes available for both pulse types in practice. Based on the RESPDOR NMR experiments shown below, the maximum rf-amplitude that can safely be applied for the PM-saturation pulse was found at $\nu_{RF}=20$ kHz, while the WURST-80 pulse with $\Delta=450$ kHz allowed for the use of higher amplitudes, defined by $\nu_{RF}=30$ kHz. Exceeding these values resulted in pronounced power reflection, which may potentially damage the spectrometer hardware. Detailed simulations of the saturation performances are given in the Supporting Materials section. Thus, a comparison of the respective saturation performances clearly indicates that WURST-80 pulses are
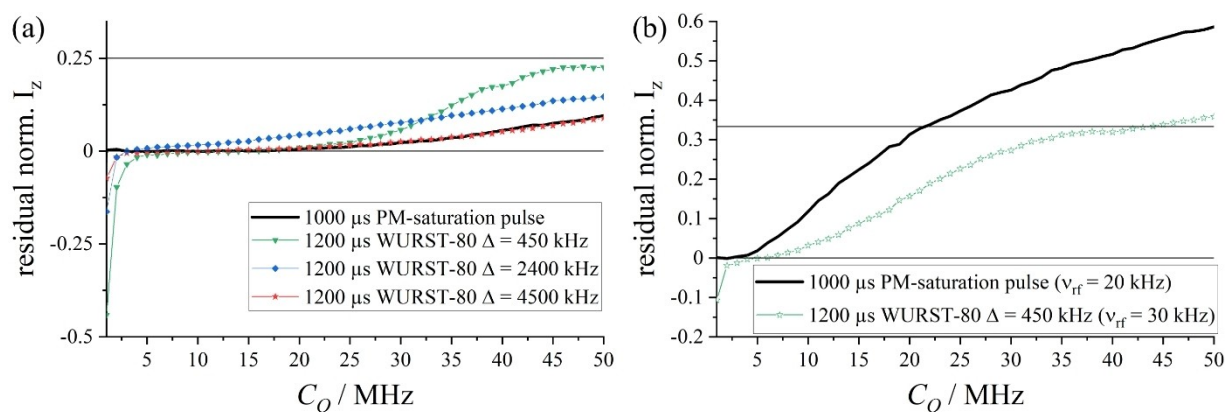
Figure 4. Numerical simulations of the saturation performances for a 1000 μs PM-saturation pulse and 1200 μs WURST-80 pulses with distinct parameter combinations (see figure legend) for various quadrupolar coupling constants, performed for a ^{27}Al species at 7.05 T ($\nu_0(^{27}$Al)=78.23 MHz), and $\nu_{rot}=10$ kHz. (a) The rf-amplitude for all pulses was set equally, corresponding to $\nu_{rf}=50$ kHz. (b) Rf-amplitudes corresponding to those applied in RESPDOR NMR experiments (see below) were used.

Chemistry–A European Journal

Full Paper
doi.org/10.1002/chem.202102113

**Chemistry Europe**
European Chemical
Societies Publishing

preferred under such conditions, keeping the residual S-spin polarization below one-third (black horizontal line).

Figures 5 and S2 summarize the results obtained on the representative samples **2**, **3**, **5**, **6**, **7**, and **8 a,b**. To get an appreciation of the accuracy and precision of the experimental data and their uncertainties, they are compared with simulations based on the crystallographically known Al···P distances. Figures 5 and S2 also show additional simulated curves spanning a range of dipolar coupling constants of ~100 Hz. From these simulations, we can conclude that for the majority of the compounds studied the dipolar coupling constant can be determined with a precision of about 50 Hz, which corresponds to a distance variation of about 0.1 Å (for the −66 ppm resonance of compound **2** the accuracy is lower (0.2 Å)). Note that the distinct behavior of compound **5**, with its shorter Al···P distance of 2.81 Å as compared to those of the other compounds is clearly detected. While the accuracy with which the distances can be determined lies within or close to the estimated precision limits for most of the compounds, some anomalous behavior is observed for compounds **6** and **8 b**, where the method seems to fail, using either PM- or W-RESPDOR. In both of these cases, the ^{27}Al C_Q values are found to be anomalously small. A closer inspection of the data indicates that already the reference signal without recoupling decays much more rapidly than for the other samples, indicating much shorter ^{31}P spin-spin relaxation times. This may indicate some

motional dynamics in the solid state that would interfere with the experimental measurement. Line shape changes were indeed detected by measurements conducted at lower temperatures, however, the rigid lattice limit could not be reached within the experimentally accessible temperature range (T > 200 K).

Aside from these exceptions, the performances of the PM- and the W-RESPDOR sequences are about comparable, as indicated by the direct comparison shown in Figure S3. Under the given circumstances, however, the W-RESPDOR method appears preferable, because its smooth amplitude variation allows the application of higher rf amplitudes without power reflection, and due to its easier implementation on commercial spectrometers.

Finally, we point out that the new method introduced here is also widely applicable to other structural problems requiring distance measurements between spin-1/2 nuclei and highly abundant spin > 1/2 nuclei featuring strong quadrupolar interactions, leading to NMR signals that are spread out into the MHz range. Possible examples of such nuclei include ^{14}N, $^{35/37}$Cl, ^{39}K, ^{45}Sc, ^{51}V, ^{59}Co, $^{63/65}$Cu, $^{69/71}$Ga, ^{75}As, $^{79/81}$Br, ^{87}Rb, ^{93}Nb, ^{115}In, ^{127}I, ^{139}La, ^{175}Lu, ^{181}Ta, and ^{209}Bi. All that is required is an accurate knowledge of their quadrupolar coupling parameters C_Q and η_Q, which are needed for simulating the degree of saturation achieved with this W-RESPDOR method under the experimental conditions chosen. C_Q and η_Q can be obtained from the analysis
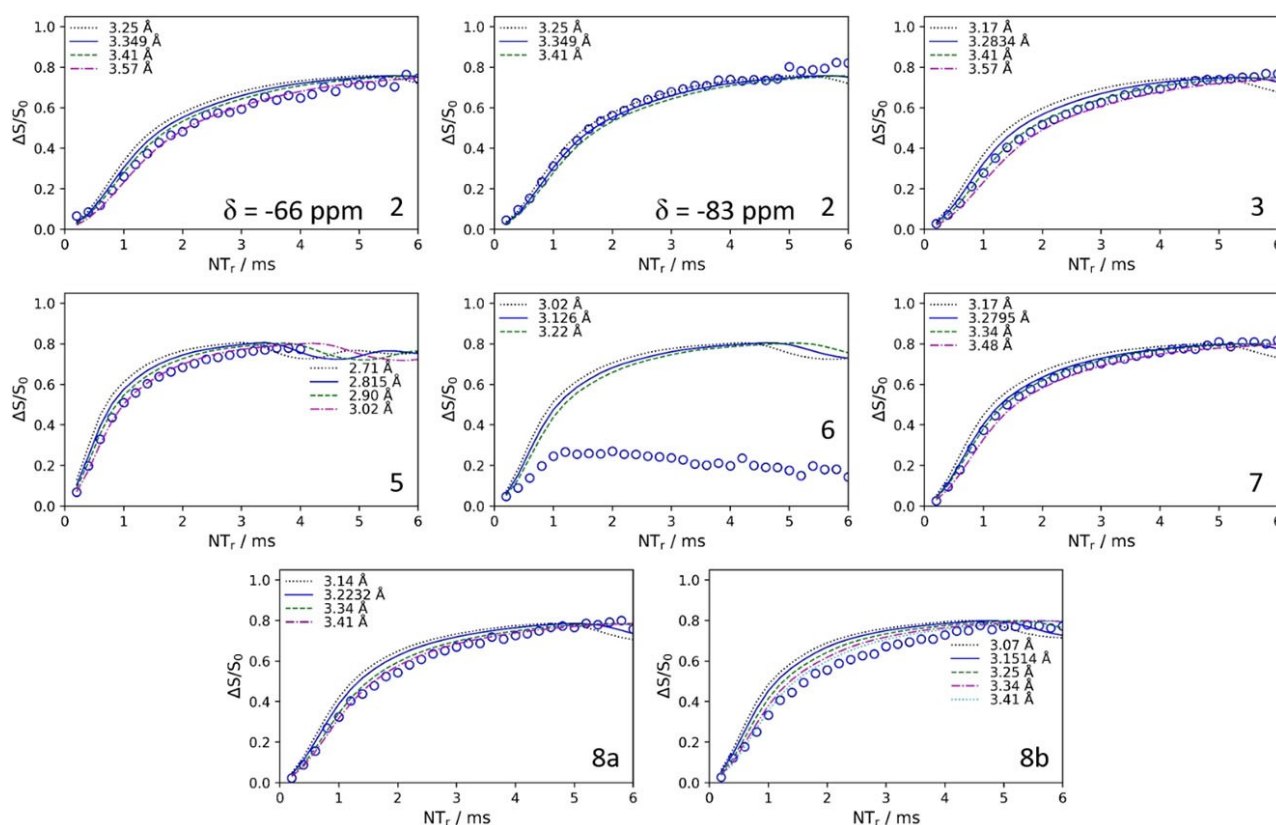
Figure 5. ^{31}P{^{27}Al} dipolar recoupling experiments, conducted on the samples under study, using RESPDOR experiments based on the W-RESPDOR scheme delineated in Figure 3. The experimental data (circles) are contrasted with simulations for different internuclear distances as indicated. The blue curves correspond to the simulation based on the crystallographic distance.

of the central transition line shape recorded by any wideband excitation method. In cases, where complete saturation can be achieved, the method can be even more powerful, as in this case no knowledge about the quadrupolar coupling parameters is required for the dipolar analysis; this feature could be particularly useful for applications to disordered and glassy systems. As noted above, the state of complete saturation may be easier to accomplish with W-RESPDOR than with PM-RESPDOR.

Conclusions

In summary, the present paper details the first comprehensive NMR characterization protocol for the study of intramolecular Al/P frustrated Lewis pairs. While ^{31}P MAS NMR spectra can be measured under standard cross-polarization (CP) conditions, the measurement of high-fidelity ^{27}Al WCPMG NMR spectra over a wide frequency range exceeding 200 kHz requires sophisticated wideband excitation methods. The NMR Hamiltonian parameters extracted from these spectra via simulation-based analysis are generally in good agreement with values computed theoretically by DFT methods. Within the present contribution, we have also introduced WURST pulses for saturation purposes that have been incorporated into dipolar recoupling experiments based on the RESPDOR approach, which we refer to as W-RESPDOR. Our results indicate that Al···P distances within the 2.8 to 3.5 Å range can be measured with good accuracy and precision in this way. With the experimental protocol developed here on a set of compounds with known crystal structures, these methods can be used for developing distance constraints in the structural characterization of other P/Al FLPs not accessible to XRD-crystallography, such as catalytic molecules incorporated into porous solids or adsorbates for applications in heterogeneous catalysis, or reactive intermediates in frozen solutions within mechanistic studies. Future applications could potentially include the characterization of intramolecular Ga-based FLP systems, which will present a considerable challenge owing to the much larger ^{71}Ga quadrupolar coupling constants. Such work is currently under consideration in our laboratories. Finally, beyond the study of FLPs, the new W-RESPDOR method introduced here has application potential for structural problems requiring distance measurements of spin-1/2 nuclei to many other high-abundance spin $>$1/2 nuclei featuring very strong quadrupolar interactions.

Acknowledgments

Conflict of Interest

The authors declare no conflict of interest.

[1] D. W. Stephan, in *Frustrated Lewis Pairs I: Uncovering and Understanding* (Eds.: G. Erker, D. W. Stephan), Springer Berlin Heidelberg, Berlin, Heidelberg, **2013**, pp. 1–44.

[2] D. W. Stephan, G. Erker, *Angew. Chem. Int. Ed.* **2010**, *49*, 46–76; *Angew. Chem.* **2010**, *122*, 50–81.

[3] D. W. Stephan, G. Erker, *Angew. Chem. Int. Ed.* **2015**, *54*, 6400–6441; *Angew. Chem.* **2015**, *127*, 6498–6541.

[4] L. Wang, G. Kehr, C. G. Daniliuc, M. Brinkkötter, T. Wiegand, A.-L. Wübker, H. Eckert, L. Liu, J. G. Brandenburg, S. Grimme, G. Erker, *Chem. Sci.* **2018**, *9*, 4859–4865.

[5] D. W. Stephan, *Science* **2016**, *354*, aaf7229.

[6] D. W. Stephan, *Chem.* **2020**, *6*, 1520–1526.

[7] A. R. Jupp, D. W. Stephan, *Trends Chem.* **2019** *1*, 35–48.

[8] G. C. Welch, R. R. S. Juan, J. D. Masuda, D. W. Stephan, *Science* **2006**, *314*, 1124–1126.

[9] G. C. Welch, D. W. Stephan, *J. Am. Chem. Soc.* **2007**, *129*, 1880–1881.

[10] P. Spies, G. Erker, G. Kehr, K. Bergander, R. Fröhlich, S. Grimme, D. W. Stephan, *Chem. Commun.* **2007**, *47*, 5072–5074.

[11] C. M. Mömming, E. Otten, G. Kehr, R. Fröhlich, S. Grimme, D. W. Stephan, G. Erker, *Angew. Chem. Int. Ed.* **2009**, *48*, 6643–6646; *Angew. Chem.* **2009**, *121*, 6770–6773.

[12] D. W. Stephan, G. Erker, *Chem. Sci.* **2014**, *5*, 2625–2641.

[13] T. Wiegand, H. Eckert, O. Ekkert, R. Fröhlich, G. Kehr, G. Erker, S. Grimme, *J. Am. Chem. Soc.* **2012**, *134*, 4236–4249.

[14] T. Wiegand, H. Eckert, S. Grimme, *Top. Curr. Chem.* **2013**, *332*, 291–346.

[15] T. Wiegand, M. Siedow, H. Eckert, G. Kehr, G. Erker, *Isr. J. Chem.* **2015**, *55*, 150–178.

[16] R. Knitsch, M. Brinkkötter, T. Wiegand, G. Kehr, G. Erker, M. Hansen, H. Eckert, *Molecules* **2020**, *25*, 1400.

[17] S. A. Weicker, D. W. Stephan, *Bull. Chem. Soc. Jpn.* **2015**, *88*, 1013–1016.

[18] L. C. Wilkins, R. L. Melen, *Small Molecule Activation with Frustrated Lewis Pairs*, Wiley, **2017**, pp. 1–24.

[19] W. Uhl, E.-U. Würthwein, *Novel Al-based FLP Systems; in "Frustrated Lewis Pairs"* (Ed. G. Erker, D. Stephan), *Topics in Current Chemistry*, Springer Verlag.

[20] G. Ménard, D. W. Stephan, *Angew. Chem. Int. Ed.* **2011**, *50*, 8396–8399; *Angew. Chem.* **2011**, *123*, 8546–8549.

[21] G. Ménard, D. W. Stephan, *J. Am. Chem. Soc.* **2010**, *132*, 1796–1797.

[22] M. A. Dureen, D. W. Stephan, *J. Am. Chem. Soc.* **2009**, *131*, 8396–8397.

[23] G. Ménard, D. W. Stephan, *Angew. Chem. Int. Ed.* **2012**, *51*, 8272–8275; *Angew. Chem.* **2012**, *124*, 8397–8400.

[24] J. Boudreau, M. A. Courtemanche, F. G. Fontaine, *Chem. Commun.* **2011**, *47*, 11131–11133.

[25] H. S. Zijlstra, J. Pahl, J. Penafiel, S. Harder, *Dalton Trans.* **2017**, *46*, 3601–3610.

[26] A. Courtemanche, J. Larouche, M. A. Legare, W. Bi, L. Maron, F. G. Fontaine, *Organometallics* **2013**, *32*, 6804–6811.

[27] C. Appelt, J. C. Slootweg, K. Lammertsma, W. Uhl, *Angew. Chem. Int. Ed.* **2012**, *51*, 5911–5914; *Angew. Chem.* **2012**, *124*, 6013.

[28] S. Roters, C. Appelt, H. Westenberg, A. Hepp, J. C. Slootweg, K. Lammertsma, W. Uhl, *Dalton Trans.* **2012**, *41*, 9033–9045.

[29] C. Appelt, H. Westenberg, F. Bertini, A. W. Ehlers, J. C. Slootweg, K. Lammertsma, W. Uhl, *Angew. Chem. Int. Ed.* **2011**, *50*, 3925–3928; *Angew. Chem.* **2011**, *123*, 4011–4014.

[30] W. Uhl, C. Appelt, J. Backs, H. Westenberg, A. Wollschläger, J. Tannert, *Organometallics* **2014**, *33*, 1212–1217.

[31] W. Uhl, C. Appelt, *Organometallics* **2013**, *32*, 5008–5014.

[32] D. Pleschka, M. Uebing, M. Lange, A. Hepp, A.-L. Wübker, M. R. Hansen, E.-U. Würthwein, W. Uhl, *Chem. Eur. J.* **2019**, *25*, 9315–9325.

[33] N. Aders, L. Keweloh, D. Pleschka, A. Hepp, M. Layh, F. Rogel, W. Uhl, *Organometallics* **2019**, *38*, 2839–2852.

[34] H. Klöcker, J. C. Tendyck, L. Keweloh, A. Hepp, W. Uhl, *Chem. Eur. J.* **2019**, *25*, 4793–4807.

[35] W. Uhl, M. Lange, A. Hepp, M. Layh, *Z. Anorg. Allg. Chem.* **2018**, *644*, 1469–1479.

Chemistry–A European Journal

Full Paper
doi.org/10.1002/chem.202102113

Chemistry Europe
European Chemical
Societies Publishing

[36] L. Keweloh, N. Aders, A. Hepp, D. Pleschka, E.-U. Würthwein, W. Uhl, *Dalton Trans.* **2018**, *47*, 8402–8417.

[37] M. Lange, J. C. Tendyck, P. Wegener, A. Hepp, E.-U. Würthwein, W. Uhl, *Chem. Eur. J.* **2018**, *24*, 12856–12868.

[38] W. Uhl, L. Keweloh, A. Hepp, F. Stegemann, M. Layh, K. Bergander, *Z. Anorg. Allg. Chem.* **2017**, *643*, 1978–1990.

[39] W. Uhl, J. Backs, A. Hepp, L. Keweloh, M. Layh, D. Pleschka, J. Possart, *Z. Naturforsch.* **2017**, *72b*, 821–838.

[40] D. Pleschka, M. Layh, F. Rogel, W. Uhl, *Phil. Trans. R. Soc. A.* **2017**, *375*, 20170011.

[41] W. Uhl, P. Wegener, M. Layh, A. Hepp, E.-U. Würthwein, *Z. Naturforsch.* **2016**, *71b*, 1043–1050.

[42] L. Keweloh, H. Klöcker, E.-U. Würthwein, W. Uhl, *Angew. Chem. Int. Ed.* **2016**, *55*, 3212–3215; *Angew. Chem.* **2016**, *128*, 3266–3269.

[43] H. Klöcker, M. Layh, A. Hepp, W. Uhl, *Dalton Trans.* **2016**, *45*, 2031–2043.

[44] W. Uhl, P. Wegener, E.-U. Würthwein, *Z. Anorg. Allg. Chem.* **2015**, *641*, 2102–2108.

[45] H. Klöcker, S. Roters, A. Hepp, W. Uhl, *Dalton Trans.* **2015**, *44*, 12670–12679.

[46] W. Uhl, P. Wegener, M. Layh, A. Hepp, E.-U. Würthwein, *Organometallics* **2015**, *34*, 2455–2462.

[47] W. Uhl, C. Appelt, M. Lange, *Z. Anorg. Allg. Chem.* **2015**, *641*, 311–315.

[48] W. Uhl, C. Appelt, A. Wollschläger, A. Hepp, *Inorg. Chem.* **2014**, *53*, 8991–8999.

[49] F. Bertini, F. Hoffmann, C. Appelt, W. Uhl, A. W. Ehlers, J. C. Slootweg, K. Lammertsma, *Organometallics* **2013**, *32*, 6764–6769.

[50] J. Boudreau, M. A. Courtemanche, V. M. Marx, D. J. Burnell, F. G. Fontaine, *Chem. Commun.* **2012**, *48*, 12250–12252.

[51] S. Roters, A. Hepp, J. C. Slootweg, K. Lammertsma, W. Uhl, *Chem. Commun.* **2012**, *48*, 9616–9618.

[52] H. Westenberg, J. C. Slootweg, A. Hepp, J. Kösters, S. Roters, A. W. Ehlers, K. Lammertsma, W. Uhl, *Organometallics* **2010**, *29*, 1323–1330.

[53] E. Kupce, R. Freeman, *J. Magn. Reson. A* **1995**, *115*, 273–276.

[54] R. Bhattacharyya, L. Frydman, *J. Chem. Phys.* **2007**, *127*, 194503.

[55] L. A. O' Dell, R. W. Schurko, *Chem. Phys. Lett.* **2008**, *464*, 97–102.

[56] L. A. O'Dell, A. J. Rossini, R. W. Schurko, *Chem. Phys. Lett.* **2009**, *468*, 330–335.

[57] R. W. Schurko, *Acc. Chem. Res.* **2013**, *46*, 1985–1995.

[58] L. A. O'Dell, *Solid State Nucl. Magn. Reson.* **2013**, *55–56*, 28–41.

[59] H. Y. Carr, E. M. Purcell, *Phys. Rev.* **1954**, *94*, 630–638.

[60] S. Meiboom, D. Gill, *Rev. Sci. Instrum.* **1958**, 29, 688–691.

[61] T. Gullion, J. Schaefer, *J. Magn. Reson.* **1989**, *81*, 196–200.

[62] L. Chopin, S. Vega, T. Gullion, *J. Am. Chem. Soc.* **1998**, *120*, 4406–4409.

[63] Z. Gan, *Chem. Commun.* **2006**, 4712–4714.

[64] X. Lu, O. Lafon, J. Trebosc, J. P. Amoureux, *J. Magn. Reson.* **2012**, *315*, 34–49.

[65] A. Goldbourt, *Magn. Reson. Chem.* **2021**, https://doi.org/10.1002/mrc.5150.

[66] E. Nimerovsky, A. Goldbourt, *J. Magn. Reson.* **2010**, *206*, 52–58.

[67] E. Nimerovsky, R. Gupta, J. Yehl, M. Li, T. Polenova, A. Goldbourt, *J. Magn. Reson.* **2014**, *244*, 107–113.

[68] E. Nimerovsky, M. Makrinich, A. Goldbourt, *J. Chem. Phys.* **2017**, *146*, 124202.

[69] M. Makrinich, E. Nimerovsky, A. Goldbourt, *Solid State Nucl. Magn. Reson.* **2018**, *92*, 19–24.

[70] J. Koppe, R. Knitsch, S. Wegner, M. R. Hansen, *J. Magn. Reson.* **2020**, *321*, 106873.

[71] R. Thakur, N. D. Kurur, P. Madhu, *Chem. Phys. Lett.* **2006**, *426*, 459–463.

[72] M. Bak, J. T. Rasmussen, N. C. Nielsen, *J. Magn. Reson.* **2000**, *147*, 296–330.

[73] R. Ahlrichs, F. Furche, C. Hättig, **2013**, University of Karlsruhe.

[74] R. Ahlrichs, M. Bär, M. Häser, H. Horn, C. Kölmel, *Chem. Phys. Lett.* **1989**, *162*, 165–169.

[75] M. Frisch, G. Trucks, H. Schlegel, G. Scuseria, M. Robb, J. Cheeseman, G. Scalmani, V. Barone, B. Mennucci, G. Petersson, et al., *Gaussian 09, Gaussian, Inc., Wallingford CT* **2009**.

[76] F. Neese, ORCA – an ab initio, density functional and semiempirical program package, version 3.0 (current development version), Max Planck Institute for Chemical Energy Conversion, Germany, **2015**.

[77] F. Weigend, R. Ahlrichs, *Phys. Chem. Chem. Phys.* **2005**, *7*, 3297–3305.

[78] S. Grimme, J. Antony, S. Ehrlich, H. Krieg, *J. Chem. Phys.* **2010**, *132*, 154104.

[79] S. Grimme, S. Ehrlich, L. Goerigk, *J. Comput. Chem.* **2011**, *32*, 1456–1465.

[80] J. Tao, J. P. Perdew, V. N. Staroverov, G. E. Scuseria, *Phys. Rev. Lett.* **2003**, *91*, 146401.

[81] K. Eichkorn, O. Treutler, H. Öhm, M. Häser, R. Ahlrichs, *Chem. Phys. Lett.* **1995**, *242*, 652–660.

[82] K. Eichkorn, F. Weigend, O. Treutler, R. Ahlrichs, *Theor. Chem. Acta* **1997**, *97*, 119–124.

[83] A. D. Becke, *J. Chem. Phys.* **1993**, *98*, 5648–5652.

[84] P. J. Stephens, F. J. Devlin, C. F. Chabalowski, M. J. Frisch, *J. Phys. Chem.* **1994**, *98*, 11623–11627.

[85] M. Kaupp, M. Bühl, V. G. Malkin, *Calculation of NMR and EPR Parameters: Theory and Applications*, John Wiley & Sons, **2006**.

[86] R. Ditchfield, *J. Chem. Phys.* **1972**, *56*, 5688–5691.

[87] S. Grimme, *J. Chem. Phys.* **2006**, *124*, 034108.

[88] D. Feller, *J. Comput. Chem.* **1996**, *17*, 1571–1586.

[89] K. L. Schuchardt, B. T. Didier, T. Elsethagen, L. Sun, V. Gurumoorthi, J. Chase, J. Li, T. L. Windus, *J. Chem. Inf. Model.* **2007**, *47*, 1045–1052.

[90] S. Adiga, D. Aebi, D. L. Bryce, *Can. J. Chem.* **2007**, *85*, 496–505.

[91] D. Massiot, F. Fayon, M. Capron, I. King, S. Le Calvé, B. Alonso, J.-O. Durant, B. Bujoli, Z. Gan, G. Hoatson, *Magn. Reson. Chem.* **2002**, *40*, 70–76.

[92] F. A. Perras, C. M. Widdifield, D. L. Bryce, *Solid State Nucl. Magn. Reson.* **2012**, *45–46*, 36–44.

[93] T. Vosegaard, H. J. Jakobsen, *J. Magn. Reson.* **1997**, *128*, 135–137.

[94] M. Haouas, F. Taulelle, C. Martineau, *Progr. Nucl. Magn. Reson. Spectrosc.* **2016**, *94–95*, 11–36.

[95] R. J. Clément, A. J. Pell, D. S. Middlemiss, F. C. Strobridge, J. K. Miller, M. S. Whittingham, L Emsley, C. P. Grey, G. Pintacuda, *J. Am. Chem. Soc.* **2012**, *134*, 17178–17185.

[96] A. Venkatesh, F. A. Perras, A. J. Rossini, *J. Magn. Reson.* **2021**, *327*, 106983.